Available online at www.sciencedirect.com
SCIENCE DIRECT®
Optics Communications 252 (2005) 150–161
OPTICS COMMUNICATIONS
www.elsevier.com/locate/optcom

Nonlinear absorption properties of 'axial-bonding' type tin(IV) tetratolylporphyrin based hybrid porphyrin arrays

P. Prem Kiran [a], D. Raghunath Reddy [b], Bhaskar G. Maiya [b], Aditya K. Dharmadhikari [c], G. Ravindra Kumar [c], D. Narayana Rao [a,*]

[a] School of Physics, University of Hyderabad, Hyderabad 500046, India
[b] School of Chemistry, University of Hyderabad, Hyderabad 500046, India
[c] Tata Institute of Fundamental Research, Colaba, Mumbai 400005, India

Received 10 September 2004; received in revised form 14 March 2005; accepted 5 April 2005

Abstract

The nonlinear absorption properties of 'axial-bonding' type hybrid porphyrin arrays based on a tin(IV) *tetratolylporphyrin (SnTTP)* scaffold are studied with picosecond and nanosecond pulses. The effect of different central metal atoms substituted adjacent to the tin(IV) porphyrin in the oligomer structure is discussed. In the picosecond regime the lifetimes of the excited singlet states and two-photon absorption (TPA) processes dominate leading to interesting switching of nonlinear absorption behaviour. The TPA cross-section (σ_{TPA}) is found to be as high as 396×10^{-46} cm^4 s photon^{-1} molecule^{-1}, for an oligomer with Sn and Ni porphyrin macrocycles. However, in the nanosecond regime the optical limiting performance has increased considerably with increasing number of porphyrins in the array and excited state absorption is found to play a major role.

PACS: 42.65.−k; 42.65.Re; 42.79.−e

Keywords: Nonlinear optics; Ultrafast processes; Optical limiting

1. Introduction

Nonlinear absorption is a phenomenon defined as an increase or decrease in the absorption coefficient with increasing intensity. The former response is called as reverse saturation of absorption (RSA), while the latter is known as saturation of absorption (SA). Organic materials with delocalized electrons are of great importance because of their large nonlinear optical absorption coefficients, architectural flexibility, and ease of

* Corresponding author. Tel./fax: +91 040 2301 1230.
E-mail address: dnrsp@uohyd.ernet.in (D.N. Rao).

0030-4018/$ - see front matter © 2005 Elsevier B.V. All rights reserved.
doi:10.1016/j.optcom.2005.04.008

fabrication. Recently materials showing RSA behaviour have been in focus for optical limiting applications [1]. SA in various materials has been studied for applications in laser pulse compression and laser amplification [2,3]. An intense laser pulse redistributes the molecular population between the ground and excited states causing a transient modification in the optical properties of the material. The dependence of transmission of organic molecules on light intensity can yield considerable information on the molecular level system that can lead to variety of nonlinear optical processes like limiting, switching and bistability. Metalloporphyrins and metallophthalocyanines form an important class of electronic materials because of the large π-electron conjugation over two-dimensional molecular structure [4,5]. Interest in advanced electronic and photonic materials recently has led to the exploration of conjugated polymers of more complex units, such as porphyrins [6]. The high polarizability and optical oscillator strength of the porphyrin macrocycles gives these materials remarkable nonlinear optical (NLO) behaviour, making them potentially useful for ultrafast switching technologies. High values of the nonlinear refractive index n_2 (which is proportional to the real part of the third order susceptibility $\chi^{(3)}$) are essential for electro-optical and all-optical switching [6], whereas high nonlinear absorption coefficients, β (proportional to the imaginary part of $\chi^{(3)}$) are important for optical limiting [7]. The architecture of the porphyrin macrocycles is important for developing materials with optimum nonlinearity and response times [8]. Structural modifications to the porphyrin ring can be expected to yield molecules with diverse photophysical and photochemical properties that will in turn affect their optical nonlinearity. This would lead to an increase in a variety of excited state processes including enhanced internal conversion and intersystem crossing (ISC), ion-association, excitation energy transfer, photoinduced electron transfer, etc. [9]. Such effects can be conveniently harnessed to enhance the third order nonlinearity and nonlinear absorption properties, hence to develop promising materials for various applications. Excited state absorption (ESA) is the most important mechanism leading to optical limiting in porphyrins [10–12]. Our group has been involved in studies on a class of porphyrins, known as tetratolylporphyrins, for achieving higher optical limiting performance and nonlinear absorption. The tetratolylporphyrins synthesized have higher third order nonlinearities [10,11,13] and efforts are being made to attain large excited state absorption cross-sections through structural modifications. In this paper, we discuss the nonlinear absorption properties of oligomers based on Sn(IV)TTP scaffold that lead to an interesting nonlinear switching behaviour.

2. Molecular structure and linear optical properties

The nomenclature of monomer and dimer molecule is *meso*-5,10,15,20-(tetratolyl) porphyrinato tin(IV) dihydroxide; [(TTP)$Sn^{IV}(OH)_2$] and [μ-[5,10,15-tri(*p*-tolyl)-20-[4-[2-[4-[10,15,20-tri(*p*-tolyl)-5-porphyrinyl]phenoxy]ethoxy]phenyl] porphyrinato]] di(tin)(IV)tetrahydroxide; [(TriTP)–$Sn^{IV}(OH)_2$]–$O(CH_2)_2O$–[(TriTP)$Sn^{IV}(OH)_2$], respectively. Dimer molecule has two monomers linked at *meso* position with ethoxy spacer. Monomer and dimer are synthesized following the procedure reported in the literature [14,15]. For simplicity we mention them as SnTTP and Sn–$Sn(TTP)_2$ in this paper. Sn^{IV} porphyrin based, 'axial-bonding' type hybrid trimers and hexamers are constructed by employing 'building-block' approach. The approach involves simple inorganic reactions such as axial bond formation of main group element containing porphyrins and insertion of metal/metalloid ions into the porphyrin cavity. The architecture of the trimer arrays [16] is such that Sn^{IV} complex of *meso*-5,10,15,20-(tetratolyl)porphyrin forms the basal scaffolding unit, the free-base, Ni^{II} porphyrins occupy the two axial sites via an aryloxy bridge. The nomenclature of the porphyrin trimer arrays discussed here is as follows: (free-base porphyrin)$_2$ (tin(IV) porphyrin) ≡ [(TTP)–$Sn^{IV}(H_2TriTP(O))_2$] and (nickel(II) porphyrin)$_2$ (tin(IV) porphyrin) ≡ [(TTP)–Sn^{IV}(Ni-TriTP(O))$_2$]. For simplicity these trimers are referred as Sn–$(H_2)_2(TTP)_3$ and Sn–$Ni_2(TTP)_3$, respectively. The scheme of construction of

hexamer arrays employs a synthetic protocol involving sequential 'organic' and 'inorganic' reactions conducted, respectively, at the peripheral *meso*-phenyl ring and the central Sn^{IV} ion of the porphyrin scaffold. The architecture of hexamers [15] are based on a covalently linked Sn^{IV} porphyrin dimer, with each of the two Sn^{IV} porphyrins centers *trans*-axially ligated to two free-base, zinc(II) porphyrins. The nomenclature of the hexamers is given as follows: [(TTP)–Sn^{IV}(H_2TriTP(O))$_2$]–O(CH_2)$_2$O–[(TTP)–Sn^{IV}(H_2TriTP(O))$_2$] and [(TTP)–Sn^{IV}(ZnTriTP(O))$_2$]–O(CH_2)$_2$O–[(TTP)–Sn^{IV}(ZnTriTP(O))$_2$]. These arrays are referred as Sn_2–$(H_2)_4(TTP)_6$ and Sn_2–$Zn_4(TTP)_6$ arrays. The molecular structure and UV–VIS absorption properties of the trimers and hexamers are reported elsewhere [15,16].

A comparison of the UV–VIS spectrum of a given trimer and hexamer with the spectra of the corresponding monomeric porphyrin suggested that the absorption peaks of these array are in the same range as those of the reference compounds. In addition, the molar absorptivities at the peak maxima (ε) values of the bands due to trimers and hexamers are nearly equal to the sum of those due to their constituent monomers. Minor variations in the spectral features of the trimers with respect to the corresponding monomers are ascribed to the 'substituent effects', i.e., differences in the axial ligands of Sn^{IV} porphyrins and the *meso* substituents of the free-base porphyrins/metalloporphyrins. These indicate that there is minimal perturbation of the electronic structures of the individual macrocyclic π-systems in these arrays. Specifically there exists no indication of the presence of exciton coupling between the porphyrin rings, i.e., basal–basal, basal–axial, or axial–axial interaction in these arrays. On the other hand, the singlet state activities of these oligomers are quite different from those of the precursor reference compounds as probed by steady-state fluorescence.

In the case of trimers, fluorescence due to both the basal and axial porphyrins is considerably quenched in comparison with that due to the monomeric chromophores. Whereas, the spectral shapes and the wavelengths of maximum emission for the individual chromophores of these arrays remains close to those due to the corresponding monomeric entities. Thus, the singlet state energy values (E_{0-0} values of H_2, Zn^{II} and Sn^{IV} porphyrins are 1.94, 2.07, and 2.04 eV, respectively) of the individual components of these arrays are assumed to be essentially similar to those of their constituent monomers. In the case of hexamers, strong quenching of fluorescence is observed. The percent quenching is close to 100, with the band that is characteristic of Sn^{IV} porphyrin emission being totally absent in the spectra. This is in contrast with the partial quenching observed in case of trimers. In trimer molecules, photoinduced electron transfer (PET) occurs from the axial porphyrin to the basal Sn^{IV} porphyrin and excitation energy transfer (EET) occurs from basal Sn^{IV} porphyrin to axial acceptors. In the case of hexamers, in addition to the EET from the basal Sn^{IV} porphyrin to its own two axial free-base acceptors, additional energy transfer from a given Sn^{IV} porphyrin to the free bases ligated at the neighbouring Sn^{IV} centers, i.e., '*trans*-axial' energy transfer is likely to occur leading to more efficient quenching. A very high efficiency of energy transfer from the basal Sn^{IV} porphyrin to the axial acceptors is observed in these axial-bonding type donor–acceptor hexamers [15] and less prominent PET reaction from axial acceptor to basal Sn^{IV} porphyrin can rationalize the 100% quenching observed for the fluorescence due to tin(IV) porphyrins of these hexameric assemblies. A generalized energy level diagram illustrating the singlet state dynamics and charge transfer (CT) states pertaining to the photoactive arrays of trimer and hexamer are reported earlier [15]. The effect of PET, EET and the CT states formed in these oligomers are found to vary the singlet state properties and these effects were considered while estimating the figures of merit for nonlinear absorption.

Fluorescence lifetimes and the respective fluorescence yields of these porphyrin molecules studied in dichloromethane as solvent are given in Table 1. Fluorescence lifetimes are measured using time correlated single photon counting (TCSPC) technique explained in the next section. All these molecules have bi-exponential decays for τ_{S_1} representing fast and slow decay. For SnTTP the lifetime is 0.562; 1 ns. In the case of trimers, τ_{S_1} has increased to 0.74 and 5.93 ns in Sn–$(H_2)_2(TTP)_3$

Table 1
Fluorescence lifetimes and % yields of Sn(IV)TTP oligomers

Porphyrin	τ_{S_1} [ns], (% fluorescence yield)
SnTTP	0.562 (71), 1 (28)
Sn–Sn(TTP)$_2$	0.57 (95), 4.94 (5)
Sn–(H$_2$)$_2$(TTP)$_3$	0.744 (71), 5.93 (28)
Sn–Ni$_2$(TTP)$_3$	0.62 (70), 2.13 (29)
Sn$_2$–(H$_2$)$_4$(TTP)$_6$	0.454 (28), 1.95 (23), 7.25 (47)
Sn$_2$–Zn$_4$(TTP)$_6$	0.667 (30), 1.73 (69)

trimer and with metal substitution in case of Sn–Ni$_2$(TTP)$_3$ τ_{S_1} is ~0.62 and 2.13 ns. As the array is becoming larger, the contribution of slowly decaying (long lived) component has increased. In case of Sn$_2$–(H$_2$)$_4$(TTP)$_6$, S_1 has a tri-exponential decay with 0.454, 1.95 and 7.25 ns whereas for Sn$_2$–Zn$_4$(TTP)$_6$ it is a bi-exponential decay of 0.667 and 1.73 ns. The lifetimes of the first excited singlet state have varied considerably with the metal substitution in hexamers. Substitution of Zn as central metal atom in porphyrin ring is reported to vary the singlet state properties and triplet state

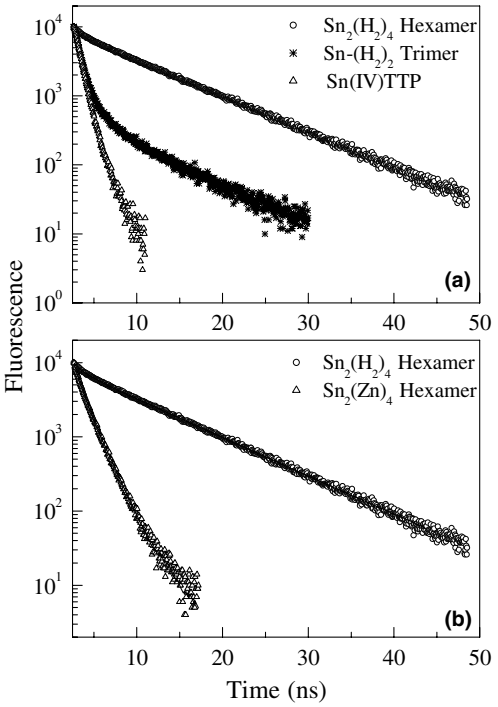

Fig. 1. Fluorescence decay curves for (a) Sn(IV)TTP monomer, Sn–(H$_2$)$_2$ trimer and Sn–(H$_2$)$_4$ hexamer and (b) Sn$_2$–(H$_2$)$_4$ hexamer and Sn$_2$–Zn$_4$ hexamer.

formation quite significantly [17]. As the excitation pulse is 6 ns, the longer S_1 lifetime of Sn$_2$–(H$_2$)$_4$(TTP)$_6$ will help in enhanced ESA and ISC, which lead to better optical limiting performance. Fluorescence decay curves for tin monomer, trimer, hexamer having Sn and H$_2$ as two centers are shown in Fig. 1(a). Fig 1(b) shows the variation in the fluorescence lifetimes with the substitution of Zn in the hexamer array. PET and EET are found to be responsible for the observed variation in the singlet state properties. PET from ground-state free-base porphyrin to the singlet-state Sn^{IV} porphyrin leads to a charge transfer state of $Sn^{IV}P^{-}$–H_2P^{+} and involves free-energy changes leading to formation of charge transfer states. These charge transfer states lead to delocalization of singlet states and the fluorescence emission wavelength is red shifted quite considerably.

3. Experimental details

Fluorescence lifetime of the fluorphores is measured using various methods. Among all, time correlated single photon counting (TCSPC) is rated as the best method. TCSPC is a digital technique, which counts the photons that are time correlated with the excitation pulse. The heart of the method is a time-to-amplitude converter. A mode locked Tsunami picosecond laser second harmonic (405 nm, FWHM ~1.2 ps) operated at 4 MHz is used as the excitation source. The decay measurements are done using a fluorescence lifetime spectrometer (Model 5000U, IBH, UK). The excitation beam is focused onto the sample and fluorescence is collected at right angles to the excitation beam and is detected by a MCP-PMT (Hamamatsu R3809U) after passing through a monochromator. Signal from the PMT is fed to the discriminator and the output of the discriminator is used as a stop signal for TAC (time to amplitude converter). The start signal is derived from the high-speed silicon detector (Thor Labs Inc., DET210). The photodiode signal is converted to TTL by pulse converter (IBH, Model TB-01) and the output is used as a start pulse for TAC. The TAC output is fed to the MCA card (Oxford Corp., UK). Repetitive laser pulsing and emitted

photon collection produced a histogram of time versus counts, representing the fluorescence decay. The data analysis is carried out using the software provided by IBH (DAS-6) that is based on reconvolution technique incorporating iterative nonlinear least square methods.

Frequency doubled Nd: YAG lasers with 25 ps and 6 ns pulse widths, 10 Hz repetition rate are used for the nonlinear absorption experiments. The porphyrin solutions in chloroform are used for the experimental studies. Open aperture *Z*-scan [18] studies are carried out by focusing the input beam on to the sample with linear transmission of approximately 75% at 532 nm using lenses of 500 mm and of 125 mm focal length to 60 and 30 μm spot size at focus in case of 25 ps and 6 ns pulses, respectively, and the transmitted light is collected with a fast photodiode. The peak fluences used in the *Z*-scan experiments with 25 ps pulses are approximately in the range of 5–52 GW cm^{-2}. The standard *f*/5 geometry is used for the optical limiting studies [19]. The linear transmission of the porphyrin solutions is approximately 70–75% for 1-mm path length of the sample at the excitation wavelength. The input fluence is varied in the range of 30 μJ cm^{-2} to 70 J cm^{-2} in the nanosecond regime. The optical limiting and *Z*-scan studies are performed at the concentration of $\sim 10^{-4}$ M ensuring identical concentration conditions for both picosecond and nanosecond regimes.

4. Nonlinear absorption properties

The nonlinear absorption behaviour observed in these hybrid arrays is totally different at nanosecond and picosecond timescales. In the picosecond regime the behaviour switches from RSA to SA and then again to RSA as the intensity increases. However, in the nanosecond regime all these molecules show good RSA in the intensity range studied. No switching from RSA to SA is observed with the nanosecond excitation.

4.1. Excitation by 25 ps pulses

At lower intensities for picosecond pulses these materials show only RSA. With increasing intensity an interesting changeover from RSA to SA and then back to RSA is observed. SnTTP monomer shows a regular RSA behaviour at lower concentrations (corresponding to 75–80% linear transmission at 532 nm) and at lower intensities. At higher intensities the ESA saturates and SA followed by RSA is observed as shown in Fig. 2(a). As the intensity is further increased to $\sim$38 GW cm^{-2}, the nonlinear absorption shows a sudden transition to RSA at higher intensities within SA behaviour (Fig. 2(b)). In the case of dimer, at lower intensities only RSA is observed (Fig. 3(a)), and as the intensity increases, the switching of the nonlinear absorption from RSA to SA and then back to RSA is observed (Fig. 3(b)). As the intensity increases the SA behaviour after RSA goes down and the RSA behaviour becomes more dominant.

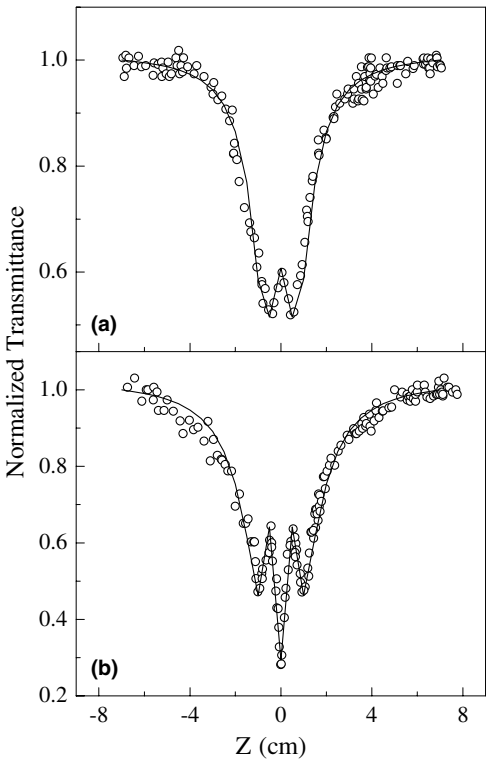

Fig. 2. Open aperture *Z*-scan curves of Sn monomer at (a) low ($\sim$14 GW cm^{-2}) and (b) high input intensities ($\sim$38 GW cm^{-2}) at lower concentration. Solid line is theoretical fit.

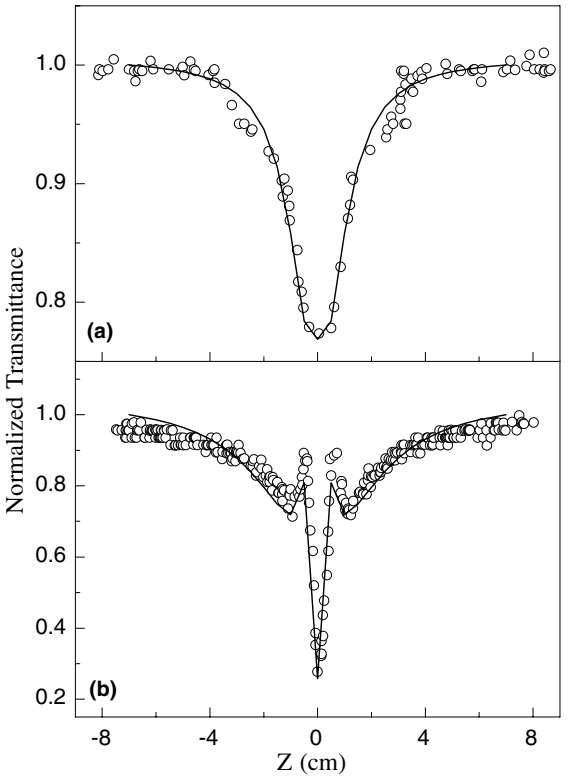

Fig. 3. Nonlinear absorption curve of Sn dimer at low concentration, at (a) 5.6 GW cm^{-2} and (b) 46 GW cm^{-2}. Solid line is theoretical fit.

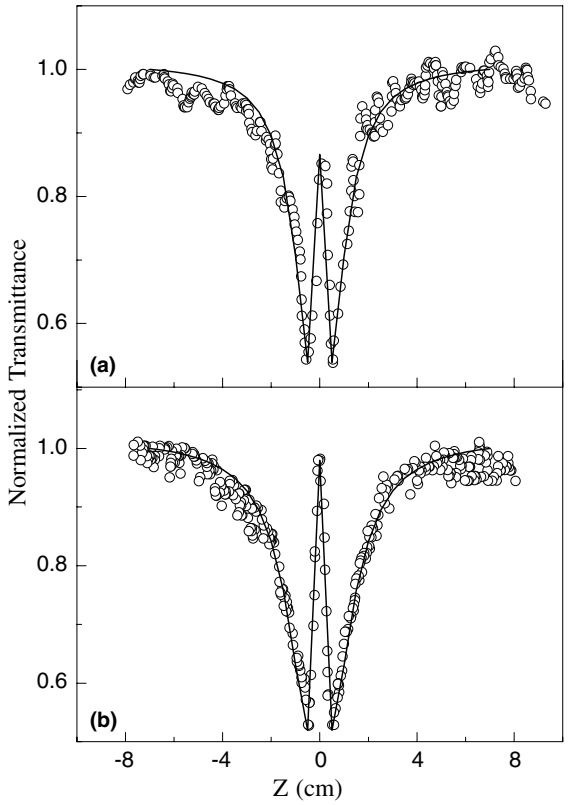

Fig. 4. Open aperture Z-scan curves of Sn–$(H_2)_2$ trimer at low concentration and at (a) 26.2 GW cm^{-2} and (b) 44.5 GW cm^{-2}. Solid line is theoretical simulation.

In the case of oligomers with Sn(IV)TTP surrounded by free-base porphyrin (H_2TTP), at lower concentrations and at lower intensities RSA is observed and with increasing intensity saturation of the ESA is observed. The saturation has increased with increasing input intensity. The open aperture Z-scan curves for Sn–$(H_2)_2(TTP)_3$ are shown in Fig. 4. Sn_2–$(H_2)_4(TTP)_6$ also shows similar behaviour and at higher intensities the saturation has increased quite considerably. While replacing H_2TTP in axial position with NiTTP lead to a total reversal in the nonlinear absorption behaviour. For Sn–$Ni_2(TTP)_3$, at lower concentrations, at lower input intensities saturation of absorption alone is observed. With gradual increase in the input intensity RSA followed by initial SA is observed (Fig. 5(a)) and at higher intensities pure RSA was observed (Fig. 5(b)). As the intensity is increased the RSA started to take over and at higher intensities RSA completely dominates due to TPA assisted ESA. At higher concentrations (60% linear transmission at 532 nm) the behaviour remained pure RSA as shown in Fig. 5(b). For Sn–$Ni_2(TTP)_3$ with 532 nm excitation falling in the edge of the absorption band, the lowest of the S_1 energy levels get excited and therefore one expects more localization of the energy leading to SA at lower intensities, whereas, at higher intensities TPA dominates and assisted by ESA shows pure RSA. However, for Sn_2–$Zn_4(TTP)_6$ at lower concentrations, a transition from SA to RSA due to two-photon/multi-photon absorption is observed. The open aperture Z-scan curve looks similar to that shown in Fig. 5(a) and with increasing intensity we observe more contribution from RSA. At higher concentrations and the intensity of

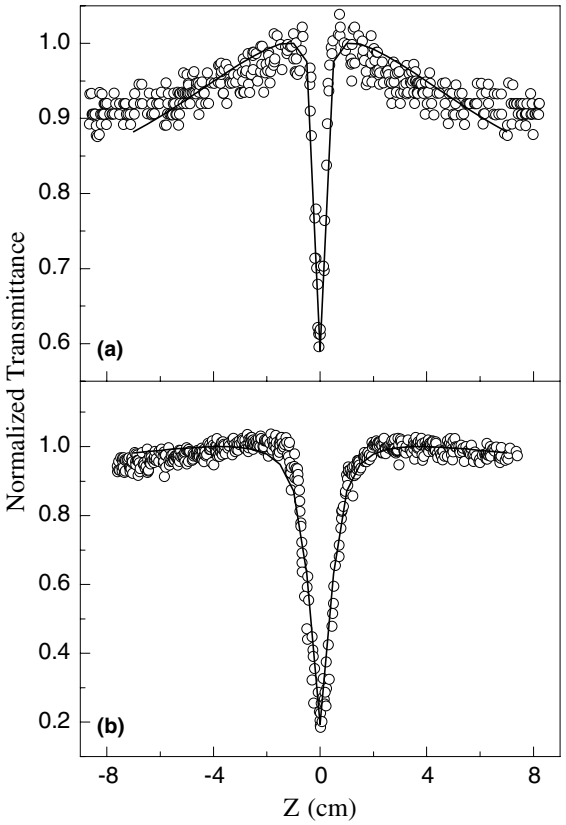

Fig. 5. Nonlinear absorption curves for Sn–Ni_2 trimer at low concentration and at intensities (a) 24.3 GW cm^{-2} and (b) 47.5 GW cm^{-2}.

28.5 GW cm^{-2}, saturation of absorption due to excited states is observed (similar to Fig. 4(a)) with transmittance at focus going up to 0.84 and the curves appear slightly broader indicating the contribution of ESA. As the intensity has increased to ~52 GW cm^{-2}, RSA is observed after saturation of absorption due to TPA (similar to that shown in Fig. 2(b)). From the open aperture *Z*-scan curves given in Fig. 2–5, it is very clear that under the similar experimental conditions, the nonlinear absorption response of these molecules is very different from that of each other, clearly indicating the effect of the presence of different central metal atoms in the porphyrin oligomer structures. Further if the nonlinear absorption is due to the solvent at higher intensity due to fifth order or higher order processes, we will not observe the saturation behaviour in the curves at the focal point (Fig. 4). This is an indirect confirmation that the observed behaviour is due to the saturation of the higher excited states of the porphyrins molecule. In order to confirm that the nonlinear absorption at higher intensities are due to the porphyrins and not due to the solvent, we carried out the *Z*-scan studies in pure solvent at intensity ranges of 10–52 GW cm^{-2}. The observed RSA behaviour at the focal point is negligible compared to the signals seen with the porphyrins solution (2% variation compared to 50% variation in porphyrins) and the effect of the solvent has been accounted for in all calculations. Though the ESA, TPA and the lifetimes of the higher excited states appears to play an important role in the nonlinear absorption of all these oligomers, TPA is more dominant in oligomers having metal–metal porphyrin macrocycles (Sn–Ni, Sn–Sn, Sn–Zn) and is absent in molecules having metal–free-base porphyrin interaction.

Observations of RSA at lower intensities and then SA due to saturation of ESA with picosecond pulse excitation has been reported earlier in cadmium texaphyrin [20] and in HITCI [21,22]. Depending on the input pulse duration, nonlinear absorption in these materials normally occurs through transitions from $S_0 \rightarrow S_n$ states by instantaneous TPA or from $S_0 \rightarrow S_1 \rightarrow S_n$ states by a two-step resonant ESA (if $S_1 \rightarrow S_n$ occurs after vibrational transitions or diffusion within the singlet states) or $T_1 \rightarrow T_n$ states by means of ESA. From the equilibrium level S_1 the molecules may relax radiatively or nonradiatively to the ground state or transfer to the lower level of triplet manifold, T_1. Efficient RSA for picosecond pulses requires that the recovery rate from the S_1 state be slow compared to the optical pumping rate. Intra-band vibrational relaxation times also play an important role for RSA. The higher excited states of the singlet manifold relax to the lower vibrational states, leading to absorption of the pump from the lower singlet sublevels to the higher excited states through ESA. In metalloporphyrins, N and L bands exist at higher energies (317 nm) in addition to the low energy B and Q bands. The N and L bands are more prominent in SnTTP compared to NiTTP and ZnTTP, whereas in

H_2TTP, N and L bands are not prominent. At higher excitation intensities, the possibility of resonant two-photon transition to the N, L bands from the lower singlet states increases. At the intensities and the pulse width used one need to consider the effect of multi-photon absorption (MPA) also. Although MPA in some of the aromatic hydrocarbons like benzene and toluene is predicted and later observed experimentally leading to nonlinear absorption, we have not observed any significant nonlinear absorption in the chloroform solvent used. Two-photon and three-photon processes leading to optical limiting are well reported in various organic compounds [23]. For porphyrins the intersystem crossing time (τ_{ISC}), which is of the order of few nanoseconds in general and few hundreds of picoseconds in some specific cases, is of minor consequence because of the 25 ps pulse width of the laser. For the picosecond excitation we therefore can neglect intersystem crossing and hence the contribution of the T_1 state, which makes the singlet states responsible for the observed behaviour at these time scales.

The values of excited state parameters σ_{ex}/σ_0, TPA coefficient (β in cm GW^{-1}), TPA cross-section (σ_{TPA}) and τ_{sn} are estimated using a generalized five-level model and from the rate equations. The generalized five-level model effectively becomes a three-level model for picosecond pulse excitation as the contribution from the triplets can be neglected, since the intersystem crossing from singlet to triplet state is very less. The differential equations are first de-coupled and then integrated over time, length, and along the radial direction, and then are solved numerically using Runge–Kutta fourth order method. Assuming the input beam to be a Gaussian, the limits of integration for r, t, and z are varied from 0 to ∞, $-\infty$ to ∞, and 0 to L (length of the sample), respectively. Typical number of slices used for r, t, and z are 60, 30, and 5, respectively. σ_1, σ_{ex}, β and τ_{ISC} are then estimated through least square fit of the experimental data [24]. The lifetime of the higher excited singlet state S_n (τ_{Sn}) has been evaluated and the lifetimes of the first excited singlet state is taken as given in Table 1. Table 2 gives the absorption cross-section and lifetime of the excited states and the TPA coefficient (β) and cross-section (σ_{TPA}). The TPA cross-section is calculated using the relation [25] $\beta = \frac{N_0}{h\nu}\sigma_{TPA}$; where h is the Planck's constant, ν is the frequency of light, and N_0 is the number molecules per unit volume. From the Table 2 it is clear that the TPA cross-section is large and comparable with the values of 11,000 GM (1 GM = 10^{-50} cm^4 s photon^{-1} molecule^{-1}) reported with dendrimer molecules comprising 29 repeat units [26]. The most plausible explanation for such a large TPA cross-section in our case is due to the fact that PET, EET and '*trans*-axial' energy transfer processes occurring simultaneously in the same porphyrin oligomeric structure leading to more delocalization of the singlet states thereby causing considerable changes in the absorption from the S_1 to the S_n states, which follows the square law for intensity dependence, leading to enhanced TPA. Such a delocalization can further enhance TPA assisted by ESA from the singlet states. Such drastic enhancement of TPA in porphyrins has been reported due to the resonant absorption and with the substitution of electron accepting groups [27,28]. Out of the different oligomers studied, the trimer having Sn, Ni porphyrins linked axially has very high σ_{TPA}. This could be due to the fact that the excitation wavelength is in resonance with the S_0–S_1 transition thus increasing the possibility of ESA assisting TPA.

The lifetimes of the excited singlet states (τ_{Sn}) are evaluated using theoretical fits (Table 2). All these oligomers are found to have the excited states relaxing in few picoseconds to few hundreds of picosecond and compare well with the reports in the literature. Sn–H arrays show longer

Table 2
Excited state parameters σ_1/σ_0, τ_{sn} and TPA coefficient β with 25 ps pulse excitation

Porphyrin	(σ_1/σ_0)	τ_{Sn} (ps)	β (cm GW^{-1})	σ_{TPA}[a] (10^{-46} cm^4 s)
SnTTP	18.32	60	0.45	2.7
Sn–Sn(TTP)$_2$	3.00	7.5	1.50	13.6
Sn–$(H_2)_2$(TTP)$_3$	3.13	500	–	–
Sn–Ni_2(TTP)$_3$	35.70	50	1.45	396.0
Sn_2–$(H_2)_4$(TTP)$_6$	1.93	500	–	–
Sn_2–Zn_4(TTP)$_6$	2.39	15	0.90	15.7

[a] The error in the σ_{TPA} is 10%.

$\tau_{Sn} \sim 500$ ps whereas rest of the molecules shows faster τ_{Sn}. Ultrafast relaxations of the order of few hundred femtoseconds are well known in porphyrin-acceptor systems due to electron transfer [29]. Photoinduced charge separation, thermal charge recombination electron transfer due to porphyrin localized charge transfer character in a directly linked pyromellitimide-(porphyrinato) Zn(II) complex and similar donor–acceptor systems are reported to be in the timescales of 770 and 5200 fs [30]. Competition between internal conversion and energy transfer in the upper excited singlet state of the porphyrin-ruthenium complexes are also reported [31]. Lammi et al. [32] reported energy and charge transfer between the adjacent states leading to excited state quenching at timescales $\leqslant$11 ps and between different sites by super exchange assisted energy transfer at timescales of $\leqslant$55 ps in diphenyl ethyne linked porphyrin dyads and triads and the relaxation rates can be tuned using the porphyrin-linker connection motif. Ultrafast excitation energy transfer processes are observed to be in the order of 12 ± 3 ps in Zn(II) porphyrin box [33]. Increasing number of porphyrin units has also reported to accelerate the relaxation dynamics of the lowest excited states from 4.5 ps for dimer to 0.3 ps for hexamer [34]. O'Keefe et al. [35] reported a two-component decay, of approximately 700 fs and 170 ± 50 ps due to exciton–exciton annihilation and exciton diffusion to recombination centers on the polymer chain from femtosecond transient photoinduced transmission measurements on Zinc conjugated porphyrin polymer. Similar faster decay of 13 ± 5 ps is also reported for dimer [35] due to the rotational diffusion of the excited molecule in solution. Relaxations of $\sim$6 ps are also reported in ethylene bridged side-to-side OEP porphyrin dimer [36]. Excited-state energy transfer is reported to be operative at timescales of 3.5 and 10 ps in *p*-phenylene linked porphyrin dimers [37], which varies with the bridge linker. Ultrafast kinetics of a hexameric benzo-porphyrin compound investigated by femtosecond transient absorption spectroscopy, shows that in the hexamer a 20 ps decay component is present which is attributed to an intramolecular interchromophoric excited-state process [38]. In cofacial lanthanide porphyrin macrocycles two relaxation processes with time constants of $\sim$1.5 and 10 ps are reported [39]. Energy transfer to the nearest porphyrin in chelate assembly separated by approximately 15–18.5 Å is reported to occur in $\sim$10 ps, which varies with the separation [40].

4.2. Excitation by 6 ns pulses

With 6 ns pulse excitation the nonlinear absorption behaviour is completely different compared to that observed with 25 ps pulses. OL curves for monomer SnTTP, trimer Sn_2–$(H_2)_2(TTP)_3$ and hexamer Sn_2–$(H_2)_4(TTP)_6$ at $\sim$75% linear transmission at 532 nm shown in Fig. 6 clearly indicates the enhanced limiting behaviour as one moves to higher homologues. Fig. 7(a) and (b) shows the variation in the limiting curves for SnTTP and Sn–Sn$(TTP)_2$ at different linear transmissions of 85% and 70%. With the introduction of heavier metalloporphyrin in the axial position in place of free-base porphyrin, in trimer and hexamer donor–acceptor homologues, lead to slightly reduced limiting response. OL curves for hexamers with free-base and Zn porphyrins in axial position are shown in Fig. 8. Though the limiting threshold has not varied greatly, the onset of limiting varies certainly, with lower values for the oligomers. Throughput fluences from these hybrids are as

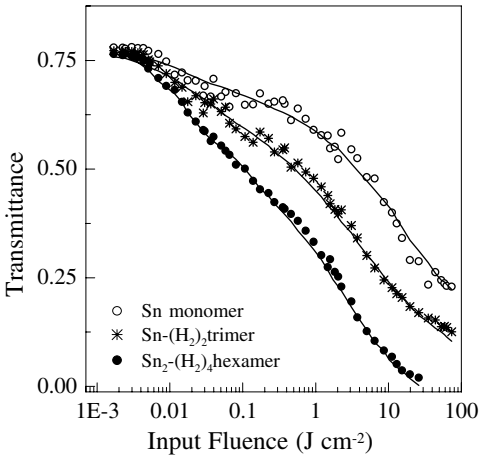

Fig. 6. Optical limiting curves of Sn(IV)TTP monomer, trimer and hexamer at 75% linear transmission with 6 ns pulses. Lines show the fits to the limiting curves.

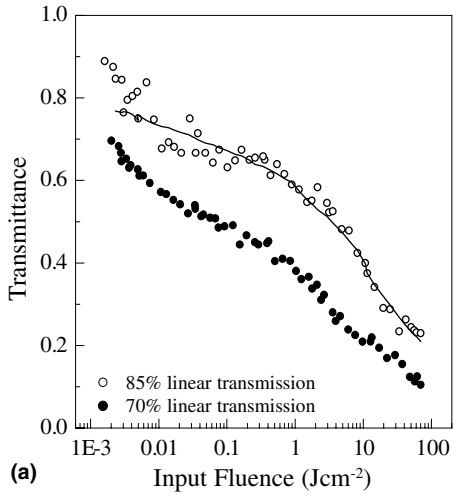

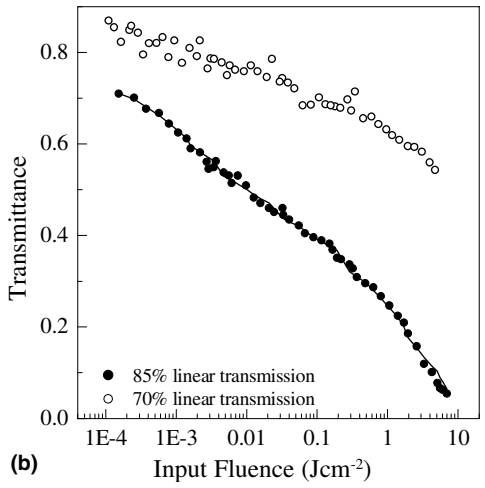

Fig. 7. OL curves of (a) Sn(IV)TTP monomer and (b) Sn–Sn dimer at 85% and 70% linear transmission. Sold lines show theoretical fits.

low as 35–52 mJ cm^{-2} with input fluences in the range of ~26–74 J cm^{-2} making these arrays very good optical limiters at higher intensities. Decreasing linear transmission to ~60%, we are able to achieve much better limiting performance in all these molecules. With increase in the concentration the ESA increases, thereby leading to improved nonlinear absorption behaviour. No aggregation is observed in the porphyrin solutions even at higher concentrations and we have not observed any scattering due to thermal blooming of the solution.

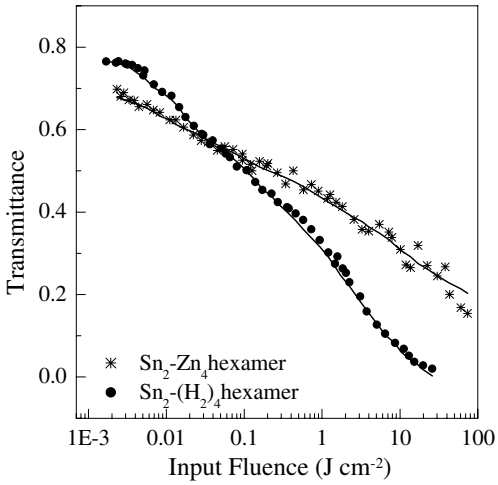

Fig. 8. OL curves showing the effect of heavier metalloporphyrin with in hexamer arrays. Solid lines show theoretical fits.

Limiting threshold values for the oligomers with 6 ns pulses are shown in Table 3. Figure of merit (σ_{ex}/σ_0), which describes the capability of a material for optical limiting, and τ_{ISC} estimated from the theoretical fits is also given in Table 3. The contribution from all the processes like PET and EET and both the radiative and nonradiative processes towards the lifetimes are taken as the effective singlet lifetime used in the rate equations. Singlet state lifetime and the ESA from $S_1 \rightarrow S_n$ in addition to $T_1 \rightarrow T_n$ are found to be responsible for the enhanced limiting performance of higher homologues. Simultaneous occurrence of strong EET and less prominent PET lead to a drastic change and stabilization of S_1 states in these molecules, making the S_1 state metastable in comparison with the excitation laser pulse width. The

Table 3
Limiting threshold and excited state parameters of the SnTTP arrays having 75% linear transmission, with 6 ns pulse excitation at 532 nm

Porphyrin	$I_{1/2}$ (J cm^{-2})	σ_{ex}/σ_0	τ_{ISC} (ps)
SnTTP	12.30	3.24	1000
Sn–Sn(TTP)$_2$	0.16	21.53	180
Sn–(H$_2$)$_2$(TTP)$_3$	2.91	7.26	380
Sn–Ni$_2$(TTP)$_3$	3.46	6.21	550
Sn$_2$–(H$_2$)$_4$(TTP)$_6$	0.46	19.45	220
Sn$_2$–Zn$_4$(TTP)$_6$	1.16	6.73	600

effective ESA cross-sections from both singlets and triplet states is taken as σ_{ex}. Even though the contribution due to ESA from S_1 to S_n is present in these molecules as the lifetime of S_1 is longer and comparable to laser pulse width, due to the low fluorescence yields most of these molecules seem to transfer to T_1 with a time given by the longer decay. However high triplet yields in these molecules indicate that intersystem crossing plays an important role in these systems at the nanosecond timescales. Such a large intersystem crossing rate has been reported in the unaggregated solutions of edge linked zinc porphyrin oligomers [41] and in monomer, dimer and polymer films [42]. The intersystem crossing time obtained from the theoretical fits is around 180–600 ps for these oligomers. Similar decay times are reported in zinc porphyrin oligomers [43] obtained from pump-probe measurements using a 0.8 ps pulse. Highly efficient triplet–triplet energy transfer and enhanced intersystem crossing is reported in rigidly linked metal and free-base porphyrin hybrids [43] and also in porphyrins linked via Ruthenium complex [44]. As the excitation pulse is of 6 ns duration, the longer lifetimes of S_1 in these arrays will help in enhanced ESA from the S_1 states, in addition to the ESA from the triplet states, which lead to better optical limiting performance. With the introduction of ZnTTP in hexamer and NiTTP in trimer in the place of the free-base TTP, we have observed reduced limiting performance of the molecule, due to the variation in the singlet state properties. When compared with the H_2TTP, NiTTP and ZnTTP monomers these oligomers show a better limiting performance under the similar experimental conditions.

5. Conclusions

The nonlinear absorption processes of porphyrin arrays based on Sn(IV) scaffold are studied in the picosecond and nanosecond timescales. In the picosecond regime, these molecules show SA at higher intensities after the initial RSA at lower intensities. At very high intensities RSA again dominates due to TPA. The lifetimes of the excited singlet states and the presence of TPA are found to be leading to the observed behaviour. Though the cross over from RSA to SA and back to RSA is observed in these hybrid arrays, the Sn–Ni_2(TTP)$_3$ has shown predominantly RSA which makes it a useful material for picosecond optical limiting. In the nanosecond regime, the optical limiting performance has increased as one move to higher homologues. Within trimer and hexamers, substitution of heavier metalloporphyrin in the axial positions has reduced the limiting performance slightly. Whereas, linearly linked Sn–Sn dimer showed a better limiting performance than the axial-bonding type trimers and hexamers. Such a crossover from RSA to SA and then back to RSA with 25 ps pulses and large TPA cross-section makes these materials potential candidates for various intensity dependent ultrafast nonlinear optical switching purposes.

Acknowledgements

Financial support from the Department of Atomic Energy – Board of Research in Nuclear Sciences, and the Defence Research Development Organization, India, is acknowledged. P.P. Kiran thanks the Council for Scientific and Industrial Research, India, for the Senior Research Fellowship. We thank National Center for Ultrafast Processes (Chennai, India) for extending us picosecond fluorescence lifetime measurement facility.

References

[1] R.C. Hollins, Curr. Opin. Solid State Mater. 4 (1999) 189.
[2] M. Hercher, Appl. Opt. 6 (1967) 947.
[3] A. Dienes, J.P. Heritage, C. Jasti, M.Y. Hong, J. Opt. Soc. Am. B 13 (1996) 725.
[4] P.N. Taylor, J. Huuskonen, G. Rumbles, R.T. Aplin, E. Williams, H.L. Anderson, Chem. Commun. (1998) 909.
[5] S.M. O'Flaherty, S.V. Hold, M.J. Cook, T. Torres, Y. Chen, M. Hanack, W.J. Blau, Adv. Mater. 15 (2003) 19.
[6] T.E.O. Screen, K.B. Lawton, G.S. Wilson, N. Dolney, R. Ispasoiu, T. Goodson III, S.J. Martin, D.D.C. Bradley, H.L. Anderson, J. Mater. Chem. 11 (2001) 312.
[7] C.W. Spangler, J. Mater. Chem. 9 (1999) 2013.
[8] J.-H. Chou, M.E. Kosal, H.S. Nalwa, N.A. Rakow, K.S. Suslick, in: K. Kadish, K. Smith, R. Guilard (Eds.), The

Porphyrin Handbook, vol. 6, Academic Press, New York (Chapter 41).
[9] S. Tsuchiya, J. Am. Chem. Soc. 121 (1999) 48.
[10] P.P. Kiran, N.K.M.N. Srinivas, D.R. Reddy, B.G. Maiya, A.S. Sandhu, A. Dharmadhikari, G.R. Kumar, D.N. Rao, Opt. Commun. 202 (2002) 347.
[11] P.P. Kiran, D.R. Reddy, B.G. Maiya, A. Dharmadhikari, G.R. Kumar, D.N. Rao, Appl. Opt., LPEO 41 (2002) 7631.
[12] A. Krivokapic, H.L. Anderson, G. Bourhill, R. Ives, S. Clark, K.J. McEwan, Adv. Mater. 13 (2001) 652.
[13] S.V. Rao, N.K.M.N. Srinivas, D.N. Rao, L. Giribabu, B.G. Maiya, R. Philip, G.R. Kumar, Opt. Commun. 182 (2000) 255.
[14] K.M. Kadish, Q.Y.Y. Xu, B.G. Maiya, J.-M. Barbe, R. Guilard, J. Chem. Soc., Dalton Trans. (1989) 1531.
[15] A.A. Kumar, L. Giribabu, D.R. Reddy, B.G. Maiya, Inorg. Chem. 40 (2001) 6757.
[16] L. Giribabu, T.A. Rao, B.G. Maiya, Inorg. Chem. 38 (1999) 4971.
[17] K. Kalyanasundaram, in: Photochemistry of Polypyridine and Porphyrin Complexes, Academic Press, 1992 (Chapter 13).
[18] M. Sheik-Bahae, A.A. Said, T.H. Wei, D.J. Hagan, IEEE J. Quantum Electron. 16 (1990) 760.
[19] T.J. McKay, J. Staromlynska, J.R. Davy, J.A. Bolger, J. Opt. Soc. Am. B 18 (2001) 358.
[20] J. Si, M. Yang, Y. Wang, L. Zhang, C. Li, D. Wang, S. Dong, W. Sun, Appl. Phys. Lett. 64 (1994) 3083.
[21] S. Hughes, G. Spruce, B.S. Wherrett, K.R. Welford, A.D. Lloyd, Opt. Commun. 100 (1993) 113.
[22] S.N.R. Swatton, K.R. Welford, S.J. Till, J.R. Sambles, Appl. Phys. Lett. 66 (1995) 1868.
[23] J.D. Bhawalkar, G.S. He, P.N. Prasad, Rep. Prog. Phys. 59 (1996) 1041.
[24] S.V. Rao, D.N. Rao, J.A. Akkara, B.S. De Cristofano, D.V.G.L.N. Rao, Chem. Phys. Lett. 297 (1998) 491.
[25] G.S. He, J.D. Bhawalkar, C.F. Zhao, P.N. Prasad, Appl. Phys. Lett. 67 (1995) 2433.
[26] M. Drobizhev, A. Karotki, A. Rebane, C.W. Spangler, Opt. Lett. 26 (2001) 1081.
[27] M. Drobizhev, A. Karotki, M. Kruk, A. Rebane, Chem. Phys. Lett. 355 (2002) 175.
[28] M. Drobizhev, A. Karotki, M. Kruk, N.Zh. Mamardashvilli, A. Rebane, Chem. Phys. Lett. 361 (2002) 504.
[29] M. Andersson, Tuning electron transfer reactions by selective excitation in porphyrin-acceptor assemblies, Ph.D. Thesis, Uppsala, 2000.
[30] N.P. Redmore, I.V. Rubstov, M.J. Therien, Inorg. Chem. 41 (2002) 566;
N.P. Redmore, I.V. Rubstov, M.J. Therien, J. Am. Chem. Soc. 125 (2003) 8769.
[31] A. Harriman, M. Hissler, O. Jrompette, R. Ziessel, J. Am. Chem. Soc. 121 (1999) 2516.
[32] R.K. Lammi, A. Ambroise, R.W. Wagner, J.R. Diers, D.F. Bocain, D. Holten, J.S. Lindsey, Chem. Phys. Lett. 341 (2001) 35.
[33] I.W. Hwang, H.S. Cho, D.H. Jeong, D. Kim, A. Tsuda, T. Nakamura, A. Osuka, J. Phys. Chem. B. 107 (2003) 9977.
[34] H.S. Cho, D.H. Jeong, S. Cho, D. Kim, Y. Matsuazaki, K. Tanaka, A. Tsuda, A. Osuka, J. Am. Chem. Soc. 124 (2002) 14642.
[35] G.E. O'Keefe, G.J. Denton, E.J. Harvey, R.T. Phillips, R.H. Friend, H.L. Anderson, J. Chem. Phys. 104 (1996) 805.
[36] M. Chachisvilis, V.S. Chirvony, A.M. Shulga, B. Kallebring, S. Larsson, V. Sundstrom, J. Phys. Chem. 100 (1996) 13867.
[37] S.I. Yang, R.K. Lammi, J. Seth, J.A. Riggs, T. Arai, D. Kim, D.F. Bocian, D. Holten, J.L. Lindsey, J. Phys. Chem. B 102 (1998) 9426.
[38] G. Schweitzer, G. De Belder, L. Latterini, Y. Karni, A.E. Rowan, R.J.M. Nolte, F.C. De Schryver, Chem. Phys. Lett. 303 (1999) 261.
[39] O. Bilsel, J. Rodriguez, D. Holten, J. Phys. Chem. 94 (1990) 3508.
[40] I.V. Rubstov, Y. Kobuke, H. Miyaji, K. Yoshihara, Chem. Phys. Lett. 308 (1999) 323.
[41] D. Beljonne, G.E. O'Keefe, P.J. Hamer, R.H. Friend, H.L. Anderson, J.L. Brédas, J. Chem. Phys. 106 (1997) 9439.
[42] F.M. Qureshi, S.J. Martin, X. Long, D.D.C. Bradley, F.Z. Henari, W.J. Blau, E.C. Smith, C.H. Wang, A.K. Kar, H.L. Anderson, Chem. Phys. 231 (1998) 87.
[43] M.A. Someda, Y. Kaizu, Inorg. Chem. 38 (1999) 2303.
[44] L. Flamigni, F. Barigelletti, N. Armaroli, B. Ventura, J.P. Collin, J.P. Sauvage, J.A.G. Williams, Inorg. Chem. 38 (1999) 661.